BUTTERWORTH HEINEMANN

Cryogenics **35** (1995) 203–207

0011-2275/95/$10.00

Linear network analysis of regenerator in a cyclic-flow system

B.J. Huang and C.W. Lu

Department of Mechancal Enginering, National Taiwan University, Taipei, Taiwan

Received 20 September 1994; revised 25 October 1994

A linear dynamics model of Darcy's form for a regenerator is first derived, from which a linear network analysis is employed to study the dynamic response of the regenerator in a cyclic-flow system. It is shown that the dynamic response of the regenerator is determined by the design of the load impedance $Z_2(s)$. The amplitude attenuation and phase shift between the mass flow and the pressure wave due to the effects of the regenerator configuration and the load impedance can be clearly seen from the present linear network analysis. It is found that introduction of load impedance will reduce the bandwith of a regenerator and increase the phase lag of the mass flow with respect to the pressure wave.

Keywords: regenerator; linear network model; cyclic-flow system

Nomenclature

A_{fr}	Flow area in regenerator (m^2)
A_{HT}	Surface area of regenerator (m^2)
C_v	Specific heat of gas at constant volume (J kg^{-1} K^{-1})
C_s	Specific heat of matrix (J kg^{-1} K^{-1})
p	Gas pressure (N m^{-2})
R	Gas constant (m^2 K^{-1} s^{-2})
T_f	Gas temperature (K)
T_s	Matrix temperature (K)
t	Time (s)
V_R	Total volume of regenerator (m^3)
V_o	Volume of reservoir (m^3)
x	Position (m)

Greek letters

ρ	Gas density (kg m^{-3})
ρ_s	Matrix density (kg m^{-3})
μ	Gas viscosity
ν	Kinematic viscosity (m^2 s^{-1})

Superscripts

$\bar{}$	Steady state or mean value
$\sim$	Perturbed value

A regenerator is a cold-storage element in regenerative coolers such as Stirling, pulse-tube and Gifford–McMahon coolers. The transient heat transfer in regenerators has been studied by many researchers[1–5]. Guo[6,7] studied the dynamic response of a regenerator using linear system theory, and a network model and a distributed-parameter model of the regenerator were derived. The studies focused only on the dynamic model of the regenerator. In practice, the regenerator is just one component in a system and the dynamic response of the regenerator should be analysed from the viewpoint of a dynamic system.

Huang and Lu[8] studied the dynamic characteristics of a regenerator connecting an infinite reservoir (zero impedance) and a reciprocating piston at isothermal conditions. Their study was further extended to emulate closely the practical situation in pulse-tube coolers. The dynamic response of a non-isothermal regenerator connecting a load impedance resulting from the flow resistance of a passage and the flow capacitance of a finite reservoir (*Figure 1*) is studied here using the linear network model.

Linear perturbation model of regenerator

The regenerator is an energy-storage element made from screen mesh wire or powders. Assuming one-dimensional flow, no axial conduction, an ideal gas, constant properties and an isotropic regenerator, the transient governing equa-

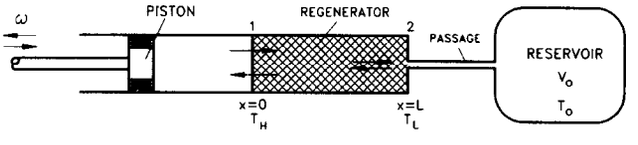

Figure 1 Regenerator system in the present study

tions can be derived from the conservation of mass, momentum and energy of the gas.

To linearize the governing equations, the inertia terms and the second-order terms in the momentum equations are neglected and a modified frictional coefficient $\bar{\alpha}$ which varies with the amplitude $\dot{m}_{max}$ of the oscillating flow, i.e. $\bar{\alpha} = f(\dot{m}_{max})$, is used to account for the pressure loss of the regenerator. The linearly perturbed equations thus can be derived by using the perturbation relations: $\dot{m}(x,t) = \bar{\dot{m}}(x) + \tilde{\dot{m}}(x,t)$; $p(x,t) = \bar{p}(x) + \tilde{p}(x,t)$; $T_f(x,t) = \bar{T}_f(x) + \tilde{T}_f(x,t)$; $T_s(x,t) = \bar{T}_s(x) + \tilde{T}_s(x,t)$:

Gas continuity equation

$$T_{ave}\frac{\partial \tilde{p}(x,t)}{\partial t} - p_{ave}\frac{\partial \tilde{T}_f(x,t)}{\partial t} + \frac{RT_{ave}^2}{A_{fr}}\frac{\partial \tilde{\dot{m}}(x,t)}{\partial x} = 0 \quad (1)$$

Gas momentum equation

$$L_F\frac{\partial \tilde{\dot{m}}(x,t)}{\partial t} + \frac{\partial \tilde{p}(x,t)}{\partial x} + R_F\,\tilde{\dot{m}}(x,t) = 0 \quad (2)$$

Gas energy equation

$$\frac{C_F}{\gamma}\frac{\partial \tilde{p}(x,t)}{\partial t} + \frac{\partial \tilde{\dot{m}}(x,t)}{\partial x} + \frac{C_T}{\gamma\tau_g}[\tilde{T}_f(x,t) - \tilde{T}_s(x,t)] = 0 \quad (3)$$

Regenerator matrix energy equation

$$\tau_s\frac{\partial \tilde{T}_s(x,t)}{\partial t} + [\tilde{T}_s(x,t) - \tilde{T}_f(x,t)] = 0 \quad (4)$$

where: the flow capacitance $C_F = A_{fr}/(RT_{ave})$; the thermal capacitance $C_T = p_{ave}A_{fr}/(RT_{ave}^2)$; the flow inductance $L_F = 1/A_{fr}$; the flow resistance $R_F = \bar{\alpha}\epsilon\nu/A_{fr}$; the gas time constant $\tau_g = \bar{\rho}\epsilon V_R C_v/(hA_{HT})$; the matrix time constant[9] $\tau_s = \rho_s(1-\epsilon)V_R C_s/(hA_{HT})$; and $\gamma = C_p/C_v$.

Solving Equations (1)–(4) by Laplace transform and substituting the following boundary conditions: $\tilde{\dot{m}}(0,s) = \tilde{\dot{m}}_1(s)$; $\tilde{\dot{m}}(L,s) = \tilde{\dot{m}}_2(s)$; $\tilde{p}(0,s) = \tilde{p}_1(s)$; $\tilde{p}(L,s) = \tilde{p}_2(s)$, we obtain the basic transfer-function model of the regenerator

$$\begin{bmatrix}\tilde{\dot{m}}_2(s)\\ \tilde{p}_2(s)\end{bmatrix} = \begin{bmatrix}\cosh[\Gamma_r(s)L] & -\frac{1}{Z_{cr}(s)}\sinh[\Gamma_r(s)L]\\ -Z_{cr}(s)\sinh[\Gamma_r(s)L] & \cosh[\Gamma_r(s)L]\end{bmatrix} \times \begin{bmatrix}\tilde{\dot{m}}_1(s)\\ \tilde{p}_1(s)\end{bmatrix} \quad (5)$$

where $\Gamma_r(s) = \sqrt{sC_{FT}(s)(R_F + sL_F)}$ and $Z_{cr}(s)$ is the characteristic impedance of the dynamic system defined as $Z_{cr}(s) = \Gamma_r(s)/[sC_{FT}(s)]$, where

$$C_{FT}(s) = C_F\frac{1 + \frac{\tau_s}{\tau_g(1+s\tau_s)}}{\gamma + \frac{\tau_s}{\tau_g(1+s\tau_s)}} \quad (6)$$

Dynamic response of regenerator in a cyclic-flow system

The dynamic response of a regenerator as shown in *Figure 1* is now considered. The regenerator connects a reciprocating piston at the hot side with a constant temperature T_H and a passage at the cold side with a constant temperature T_L. The reservoir is at a constant temperature T_o and has a fixed volume V_o. This configuration is similar to an orifice pulse-tube cooler, except that the pulse tube and the heat exchangers are not included.

Load impedance

The passage and the reservoir gives an equivalent circuit as shown in *Figure 2*. The impedance of the passage includes the resistance $R_{Ft}(s)$, inductance $L_{Ft}(s)$ and capacitance $C_{Ft}(s)$. The impedance of the reservoir is dominated by a capacitance $C_{Fo}(s)$. An equivalent load impedance $Z_2(s)$ can be defined at the exit of the regenerator: $Z_2(s) \equiv \tilde{p}_2(s)/\tilde{\dot{m}}_2(s)$, as shown in *Figure 2*.

Dynamic model of cyclic-flow system

A dynamic model of the regenerator in a cyclic-flow system expressed in Darcy's form is given by

$$G_{m_2\Delta p} \equiv \frac{\tilde{\dot{m}}_2(s)}{\Delta\tilde{p}(s)} = \frac{1}{Z_2(s)\{\cosh[\Gamma_r(s)L] - 1\} + Z_{cr}(s)\sinh[\Gamma_r(s)L]} \quad (7)$$

where $\Delta\tilde{p} \equiv \tilde{p}_1 - \tilde{p}_2$.

Effect of load impedance

The dynamic response of the regenerator in a cyclic-flow system is affected by the design of the load impedance $Z_2(s)$. For the open end, i.e. $Z_2(s) = 0$, the sizes of the passage and the reservoir are infinite. Equation (7) then becomes

$$G_{m_2\Delta p}(s) = \frac{1}{Z_{cr}(s)\sinh[\Gamma_r(s)L]} \quad (8)$$

For the closed end, i.e. the regenerator is blocked and $Z_2(s) = \infty$, $\tilde{\dot{m}}_2 = 0$ always.

The design of the passage and the reservoir can be controlled such that $Z_2(s) = Z_{cr}(s)$. The transfer function for this load-matching condition then becomes

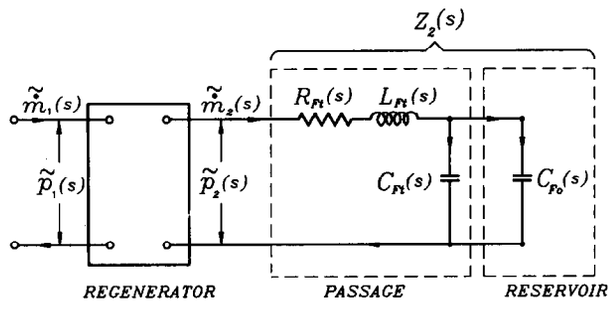

Figure 2 Equivalent circuit of the cyclic-flow system

$$G_{m_2\Delta p} = \frac{1/Z_{cr}(s)}{\{\cosh[\Gamma_r(s)L] - 1\} + \sinh[\Gamma_r(s)L]} \quad (9)$$

Dynamic response of regenerator

For illustration, let us assume the following parameters: system mean pressure P_{ave} = 15 atm (abs); T_H = 360 K; T_l = 77 K; regenerator average temperature T_{ave} = 218.5 K; piston swept volume V_P = 6.0 cm^3; piston stroke 0.7 cm; piston rod length 2.8 cm; regenerator diameter D = 1.1 cm; and regenerator length L = 5.7 cm. The modified frictional coefficient $\bar{\alpha}$ is computed using the correlations of Tanaka[10]. $\bar{\alpha}$ can be presented in terms of the cycle frequency f

$$\bar{\alpha} = \frac{175}{2\epsilon d_h^2} + \frac{0.8}{\epsilon d_h \omega} \frac{1.007784\pi V_p f \rho^*}{A_r \epsilon} \quad (10)$$

where: $\rho^* \equiv \rho(T_H)/\rho(T_{ave})$ = 0.7 in the present case; ϵ is the porosity; d_h is the hydraulic diameter defined as $d_h = \epsilon d_m/(1 - \epsilon)$; and d_m is the wire diameter.

The heat transfer coefficient h inside the regenerator is evaluated by the correlation of Tanaka[10]

$$h = 0.33 \frac{k_f}{d_h} \left(\frac{\rho d_h}{\mu} \frac{2V_p f \rho^*}{A_r \epsilon} \right)^{0.67} \quad (11)$$

where: $A_{HT}/V_R = 4(1 - \epsilon)/d_m$; $A_r = A_{fr}/\epsilon$; V_R is the total volume of the regenerator; and k_f is the thermal conductivity of gas.

Four kinds of stainless screen wire mesh are used: 150, 200, 250 and 400 mesh. The regenerator properties are evaluated using the empirical equations derived by Chang[11], and are listed in *Table 1*.

The frequency response or Bode plot of $G_{m_2\Delta p}(s)$ for the open-end configuration (Z_2 = 0) is presented in *Figure 3*. The attenuation of $\dot{m}_2$ as well as the phase shift is larger for the regenerator with a larger mesh number (i.e. denser screen). The bandwidth of $G_{m_2\Delta p}(j\omega)$ is defined at −3 db gain which specifies the cut-off frequency f_{cut}. It is seen from *Table 2* that the bandwdith is wider for regenerators with a larger mesh number. However, the phase lags at f_{cut} for the four kinds of regenerators are all small and very close, all within 4.2°. This means that a quasi-steady approximation of Darcy's law can hold within the bandwidth, both in terms of gain and phase shift, for the open-end configuration (Z_2 = 0).

The frequency response or Bode plot of $G_{m_2\Delta p}(s)$ for the load-matching configuration, i.e. $Z_2(s) = Z_{cr}(s)$, is shown in *Figure 4*. The attenuation of $\dot{m}_2$ is more rapid for the regenerator with a small mesh number. But the phase lag increases more rapidly with increasing frequency for the regenerator with large screen wire mesh (i.e. denser screen). It is seen from *Table 3* that the bandwidth of $G_{m_2\Delta p}(j\omega)$ as well as the phase lag increases with increasing mesh number (denser screen). It can be seen from *Tables 2* and *3* that the phase lag reaches a minimum value for the open-end configuration and then increases with increasing load impedance $Z_2(s)$. This indicates that the flow wave $\dot{m}_2$ will lag further behind the pressure wave $\Delta\tilde{p}$ if the load impedance $Z_2(s)$ increases.

Table 1 Regenerator properties

Mesh	150	200	250	400
d_m (mm)	0.06604	0.05334	0.04064	0.02540
ϵ	0.732	0.707	0.735	0.686
d_h (mm)	0.1803	0.1287	0.1127	0.554
α (mm^{-2})	2691.63	5281.81	6886.6	28417.0
β (mm^{-1})	4.437	6.215	7.097	14.417
A_{HT}/V_R (mm^{-1})	16.23	21.97	26.08	52.28

At the load-matching condition, the effect of regenerator impedance vanishes. The pressure as well as the mass flow wave can be propagated directly to the other side of the regenerator without loss. Under this circumstance, the pressure and mass flow wave propagation is determined by the load impedance only. The transport of mass and momentum through the regenerator have the largest efficiency. The load-matching condition is thus the optimum configuration in the cyclic-flow system. The design of the load impedance $Z_2(s)$ plays an important role in the transport phenomena of waves in the cyclic-flow system of *Figure 1*.

It can be further shown that for the open-end and load-matching configurations, the dynamic models in Darcy's form [equations (9)] are reduced to the standard steady state Darcy's equation if the cyclic flow frequency is low. That is

$$\lim_{\omega \to 0} |G_{m_2\Delta p}(j\omega)| = \frac{A_{fr}}{\bar{\alpha}\epsilon\nu L} = \frac{1}{R_F L} = \text{constant} \quad (12)$$

This indicates that a quasi-steady approximation of Darcy's law can hold within the bandwidth shown in *Tables 2* and *3*.

Realization of load impedance $Z_2(s)$

The load impedance $Z_2(s)$ for the passage and reservoir combination can be realized approximately by the flow resistance R_{Ft}, the flow capacitance C_{Ft} and the flow inductance $L_{Ft}(s)$ of the passage and the flow capacitance $C_{Fo}(s)$ of the reservoir (see *Figure 2*). Hence

$$Z_2(s) = R_{Ft} + sL_{Ft} + \frac{1}{s(C_{Ft} + C_{Fo})} \quad (13)$$

Here: $R_{Ft} = f'(L_t/d_t)v/(2A_t)$; $L_{Ft} = L_t/A_t$; $C_{Ft} = A_t L_t/(RT_t)$; and $C_{Fo} = V_o/(RT_0)$, where f' is the frictional factor of oscillating pipe flow[12], v is the mean velocity in the passage and A_t is the flow area in the passage.

For the load-matching condition $Z_2(s) = Z_{cr}(s)$, the dimensions of d_t, L_t and V_o are evaluated and listed in *Table 4*. It is seen that for the passage with diameter d_t = 0.5 mm, the required length L_t varies from 1.22 to 3.65 mm and the reservoir volume V_o varies from 7.5 to 22.9 cm^3. The passage in this case looks more like an orifice plate instead of a tube. This situation is quite similar to that of an orifice pulse-tube cooler.

Conclusions

A linear dynamic model of Darcy's form for a regenerator is first derived, from which a linear network analysis is employed to study the dynamic response of the regenerator in a cyclic-flow system. It is shown that the dynamic

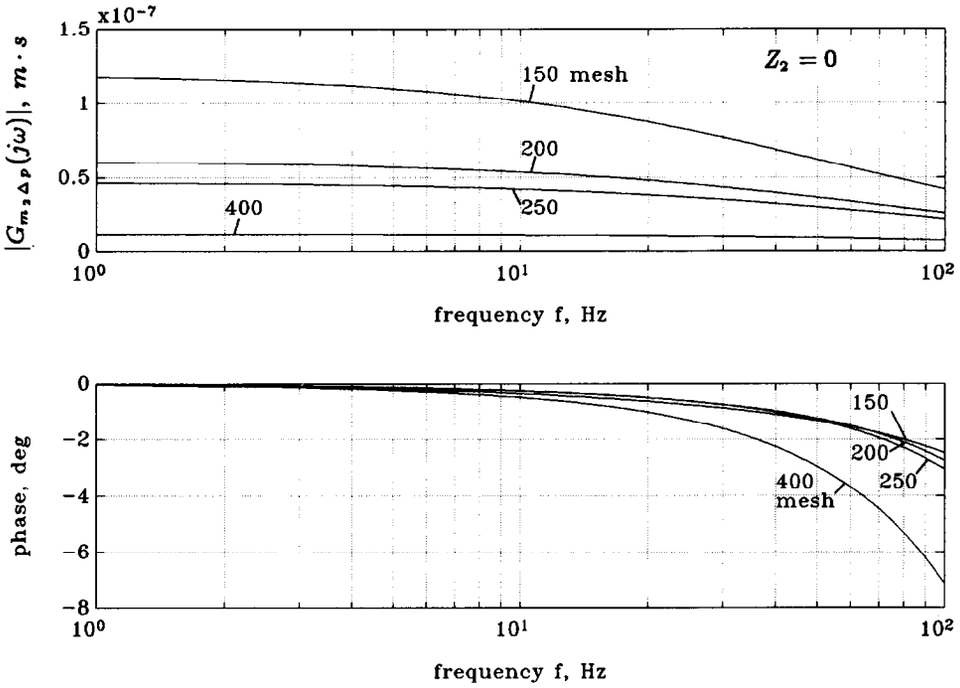

Figure 3 Bode plot of $G_{m_2\Delta p}(s)$ for open-end configuration ($Z_2 = 0$)

Table 2 Cut-off frequency of $G_{m_2\Delta p}(j\omega)$ for $Z_2(s) = 0$

Mesh	f_{cut} (Hz)	ϕ_{cut} (°)
150	22.0	−0.687
200	29.7	−0.737
250	35.2	−0.898
400	66.6	−4.20

Table 3 Cut-off frequency of $G_{m_2\Delta p}(j\omega)$ for $Z_2(s) = Z_{cr}(s)$

Mesh	f_{cut} (Hz)	ϕ_{cut} (°)
150	19.1	−2.71
200	23.9	−3.74
250	26.9	−4.48
400	34.4	−9.31

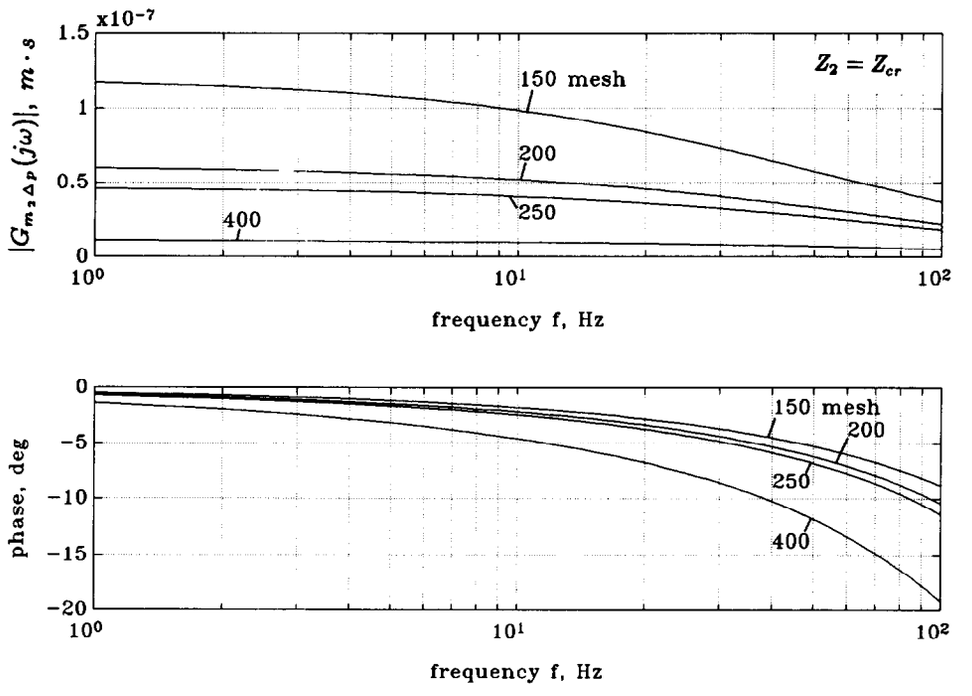

Figure 4 Bode plot of $G_{m_2\Delta p}(s)$ for matched condition ($Z_2 = Z_{cr}$)

Table 4 Load configuration for $Z_2(s) = Z_{cr}(s)$

d_t (mm)		0.2	0.5	1.0	1.25	2.0
150 mesh	L_t (mm)	0.015	1.2	33.0	100.0	944.0
	V_o (cm^3)	23.1	22.9	21.5	20.1	12.2
200 mesh	L_t (mm)	0.02	1.66	45.0	137.0	1291.0
	V_o (cm^3)	16.7	16.6	15.6	14.5	7.4
250 mesh	L_t (mm)	0.02	1.83	49.6	150.0	1417.0
	V_o (cm^3)	15.2	15.0	14.1	13.1	5.5
400 mesh	L_t (mm)	0·04	3.65	98.95	299.8	–
	V_o (cm^3)	7.5	7.4	6.9	6.2	–

response of the regenerator is determined by the design of the load impedance $Z_2(s)$. The amplitude attenuation and phase shift between the mass flow and the pressure waves due to the effects of regenerator configuration and load impedance can be clearly seen from the present linear network analysis. It is shown that introduction of load impedance will reduce the bandwidth of a regenerator and increase the phase lag of the mass flow with respect to the pressure wave. This could reduce the cooling effect in a cooler, since the phase angle between the mass flow and the pressure (or temperature) waves is not in phase. The amplitude attenuation and the phase shift of the mass flow and the pressure waves due to the effect of the regenerator are clearly shown in the present study. Control of this phenomenon is quite important in the design of regenerative-cycle coolers such as Stirling or pulse-tube coolers.

Acknowledgements

The present study was supported by the Energy Commission, Ministry of Economic Affairs, Taiwan, ROC, through Grant No. 832Z6, 1993 and the National Science Council, Taiwan, ROC, through Grant No. NSC81-0401-E002-587.

References

1 **Rea, S.N. and Smith, J.L., Jr** The influence of pressure cycling on thermal regenerators *ASME J Eng for Ind* (Aug 1967) 563–569
2 **Quale, E.B. and Smith, J.L., Jr** An approximate solution for the thermal performance of a Stirling-engine regenerator *ASME J Eng for Power: Ser A* (April 1969) No. 2, 109–112
3 **Modest, M.F. and Tien, C.L.** Analysis of real-gas and matrix-conduction effects in cyclic cryogenic regenerators *ASME J Heat Transfer* (May 1973) 199–205
4 **Modest, M.F. and Tien, C.L.** Thermal analysis of cyclic cryogenic regenerators *Int J Heat Mass Transfer* (1974) **17** 37–49
5 **Walker, G. and Vasishta, V.** Heat transfer and flow friction characteristic of dense-mesh wire-screen Stirling-cycle regenerator *Adv Cryog Eng* (1970) **16** 324–332
6 **Guo, F.Z. *et al.*** Flow characteristics of a cyclic flow regenerator *Cryogenics* (1987) **27**, 152–155
7 **Guo, F.Z.** Network model of cyclic flow regenerator for Stirling cryocooler *Cryogenics* (1990) **30** (suppl) 199–205
8 **Huang, B.J. and Lu, C.W.** Dynamic response of regenerator in cyclic flow system *Cryogenics* (1993) **33** 1046–1052
9 **Wylie, E.B. and Streeter, V.L.** *Fluid Transients* McGraw-Hill Inc., New York, USA (1978)
10 **Tanaka, M., Yamashita, I. and Chisaka, F.** Flow and heat transfer characteristics of Stirling engine regenerator in an oscillating flow *JSME Int J: Ser II* (1990) **33** 283–289
11 **Chang, W.-S.** Porosity and effective thermal conductivity of wire screens *ASME J Heat Transfer* (1990) **112** 5–9
12 **Roach, P.D. and Bell, K.J.** Analysis of pressure drop and heat transfer data from the reversing flow test facility, Argonne National Laboratory Report ANL/MCT-88-2 (May 1989)